10C.6

THE IMPORTANCE OF ATMOSPHERIC TEMPERATURE ON THE SIZE AND STRUCTURE OF TROPICAL CYCLONES

Diana R. Stovern* and Elizabeth A. Ritchie
University of Arizona, Tucson, Arizona

1. INTRODUCTION

In the months between August 2004 and October 2005, the United States endured several of the most expensive hurricanes ever to occur in U.S. history, including Hurricane Katrina in August-September 2005 and Hurricane Rita in October 2005. These storms devastated the Gulf coast with massive storm surges, torrential rains, and intense straight line winds (Beven et al. 2008). Interestingly, both of these devastating tropical cyclones underwent a dramatic expansion in the size of their wind field after crossing the warm loop current west of 83°W in the Gulf of Mexico. In particular, the wind field of Hurricane Katrina, as measured by the average radius of 34 knot winds, rapidly expanded from approximately 105 km on the 26th of August as it crossed the Florida Peninsula to a peak radius of 335 km on the 29th of August. Of note, the environment at the time of Katrina's rapid enlargement was approximately 2°C warmer from the surface through 400 mb than the environment where it initially formed as measured by ERA Interim reanalysis data. In addition, the sea-surface temperatures (SST) were 1-2°C warmer in the Gulf of Mexico than in the Caribbean. The characteristics of the atmosphere and its interaction with the underlying ocean were important in the growth of Hurricane Katrina as discussed by Beven et al. (2008). This paper will provide a look at some of the possible mechanisms that might cause TCs like Hurricane Katrina to rapidly expand into large tropical cyclones.

In this study we worked under the premise that size changes can occur due to two processes: internal mechanisms and environmental forcing. Focusing on the latter, we used a sophisticated numerical model, the Weather Research and Forecasting (WRF) model to investigate how small changes in the environment might cause changes in the size and structure of a simulated tropical cyclone. In the simulations presented, making a small change in the atmospheric temperature while keeping the sea-surface temperature constant caused significant changes in the size of the tropical cyclone wind and precipitation fields. In this paper, we will present the results of the simulations and discuss how the atmospheric temperature influenced size changes in each modeled tropical cyclone. This paper will be structured as follows: section 2 will provide the configuration of the numerical model and general aspects of the environment in which the tests were performed; results from the simulations will be shown in section 3; and the link between environmental temperature and TC size changes will be discussed in section 4. Finally, the last section will include a summary of this research and concluding remarks.

*Corresponding author address:
Diana Stovern, Department of Atmospheric Sciences, 1118 E 4th St. Tucson, AZ 85721-0081. Email: dstovern@atmo.arizona.edu.

2. METHODOLOGY

In order to achieve the goals of this project the WRF-ARW provided by the National Centers for Atmospheric Research (Skamarock et al. 2005) was used. The model was configured with a large, square parent domain (D1) of size 5373 km^2 with 27-km grid-point resolution (199x199 grid points) (Stovern and Ritchie 2012). Within D1 two vortex-following nests that were also square domains with grid-point resolutions of 9 km (D2) and 3 km (D3) were initialized. The size of these domains were 1350 km^2 (150x150 grid points) and 720 km^2 (240x240 grid points), respectively. D2 was initialized in the southeast quadrant of D1, allowing it to move freely through the simulation without reaching the western boundary of D1. All three domains were comprised of 42 vertical levels, 7 of which were below 850 hPa. In addition, all three domains had convection explicitly resolved using the WRF single-moment 6-class scheme, which includes ice, snow, and graupel processes. The two outer domains used the Kain-Fritsch cumulus parameterization scheme. Radiative processes were parameterized in all three domains using the Rapid Radiative Transfer Model (RRTM) for longwave radiation and the Dudhia scheme for shortwave radiation.

The atmosphere in the idealized environment for the control simulation was initialized following the methodology in the experiments of Frank and Ritchie (1999). Similar to those simulations, the relative humidity and virtual temperature values specified for these levels were obtained from the McBride and Zehr (1981) pre-storm composite data. Embedded within this environment was a symmetric vortex centered directly on 15° N and 135° W, with maximum winds of tropical–storm strength (64-kts), and a radius of maximum winds located 100 km from the storm center. A positive relative humidity anomaly was added in the center of the vortex to facilitate the onset of convection. The entire model atmosphere was initialized over a water world to avoid potential impacts from land. The underlying ocean was set at a constant 29° C (302 K) throughout the evolution of each storm simulation.

A number of sensitivity simulations were run in which the environmental virtual temperature profile was systematically cooled or warmed by 1 °C at a time from the control - 3 °C to the control + 3 °C. The results from the control along with the C - 3 °C (C3) and C + 3 °C (W3) simulations are presented in this paper. The change in temperature was applied over the entire vertical and horizontal extent of the atmospheric domain. As a consequence, the environments initialized with different relative humidity and specific humidity profiles. Each simulation was run for 120 hours, producing 12-hourly output in the coarse domain and 3-hourly output in the two nested domains.

3. RESULTS

The evolution of intensity and size for the three simulations is shown in figure 1. Each simulation initialized with the same minimum central pressure and maximum wind speed. For the purpose of this abstract, the intensity for each simulation is defined by the 6-hour averaged maximum wind speed (Fig. 1a). The size of the TC outer-core is defined as the radius of 64-kt winds and the overall storm size is defined as the radius of 34-kt winds (Fig. 1b, c). The radius of 64- and 34-kt winds azimuthally averaged values are plotted every 12 hours for each simulation.

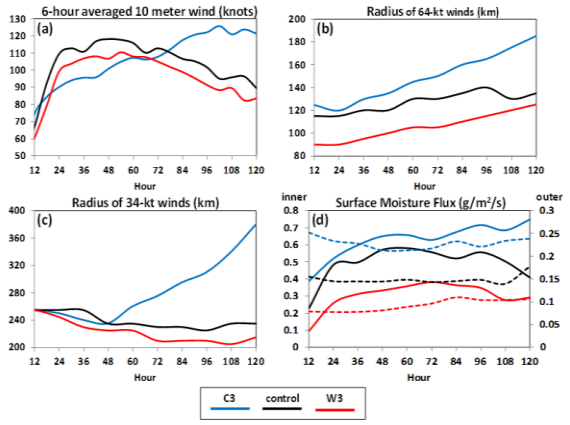

Figure 1: a) 6-h averaged maximum 10-m wind (knots); b) Radius of 64-kt winds; c) Radius of 34-kt winds; and d) upward surface moisture fluxes (g m^{-2} s^{-1}) showing inner-core fluxes (solid) and outer-core fluxes (dashed) for simulations C3, control, and W3.

In all three simulations, the storms spun up similarly in the first 12 hours of simulation. The intensities started to diverge around 24 h with the control simulation intensifying most rapidly, reaching a maximum wind speed of 118 knots after 48 hours of simulation. The warmer environment produced a storm (W3) that intensified similarly to the control through 48-h of simulation and then gradually weakened through 120 h. In contrast, C3 was the weakest TC at 48 h, but then quickly intensified after hour 72, never showing signs of decay during the entire simulation. C3 attained the strongest maximum wind speed of 126 knots at 102 h.

Interestingly, the size evolution did not display the same characteristics as the intensity evolution. The radius of 64-kts, which describes the size of the outer core, was largest in C3 as early as hour 12 and remained the largest through the end of the simulation. As a general rule, the size of the radius of 64-kt winds decreased with increasing environmental temperature. The radius of 34-kt winds was largest in the control simulation until hour 48 when C3 began to rapidly grow reaching a final radius of 380 km by 120 h of simulation. The radius of the 34-kt winds decreased for the control and W3 simulations, ending with a final value of 255 km. Clearly, the effects of the environmental temperature in the cooler environment (C3) was favorable for later TC intensification and outer-core expansion of the wind fields.

4. ENVIRONMENTAL TEMPERATURE AND SIZE CHANGES

4.1 *Moisture Fluxes*

The release of latent heat from condensation is the primary source of energy to maintain circulation in an intensifying tropical cyclone (Malkus and Riehl 1960). The thermally driven circulation relies on frictional convergence of moist fluxes of enthalpy from the sea-surface (Emanuel 1986). Moist fluxes of enthalpy are dependent on the differences in temperature and vapor pressure between the sea and air, and also the wind speed (Malkus and Riehl 1960). In these simulations, the same surface winds were used for the initial conditions, thus, changes in the surface moisture fluxes are more heavily dependent on the vapor pressure difference (e_{sea}-e_{air}) and temperature difference (T_{sea}-T_{air}).

The time evolution of the surface moisture fluxes are shown in figure 1d. The moisture fluxes are averaged between the 0 and 100 km (inner-core) and 100 to 300 km (outer-core) radii. The moisture fluxes are highest in C3 and decrease with increasing environmental temperature. The values of the inner-core fluxes are more than double that of the outer-core values and this is reflected by the intense inner-core winds. The outer-core fluxes are not as sensitive to changes in the wind field which may explain why they do not vary as much temporally as the inner-core fluxes. It seems possible that the role of the increased outer-core fluxes is to aid in the expansion of the outer-core winds (R64) and overall size (R34).

4.2 *Equivalent Potential Temperature*

The equivalent potential temperature (θ_e) changed when the virtual temperature was altered in the idealized environments. The warm simulation (W3) was initialized with the highest equivalent potential temperature in the boundary layer, and as a result, intensified rapidly in the early stages of the simulation. The intensity of the tropical

cyclone is dependent on the θ_e values inside the eyewall as described by Betts (1987). However, once the high θ_e air was depleted through convective processes in the warm simulation the moisture fluxes were not adequate to replenish the boundary layer air, and deep convection was not sustained, leading to a collapse in the eyewall convection. Conversely, C3 had relatively low boundary-layer θ_e initially along with relatively weaker inner-core convection. Eventually the high surface moisture fluxes supplemented the boundary layer θ_e, triggering deep convection and causing C3 to increase in intensity and size.

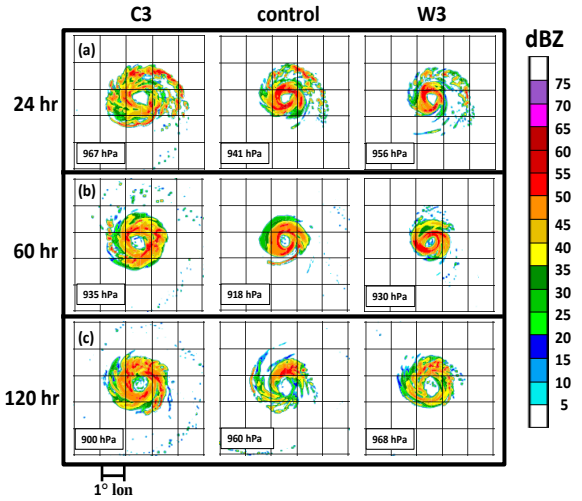

Figure 2. Radar reflectivity for the cold (C3), warm (W3), and control simulations at: a) 24 h; b)60 h; and c) 120 h of simulation. Gird boxes are 1° latitude by 1° longitude. The minimum central pressure is indicated on each panel.

4.3 *Mechanism of Surface Fluxes and Size Expansion*

Large surface fluxes increase the amount of convection and latent heating and enhance the secondary circulation of the storm. Enhanced outer-core fluxes, supplement boundary layer θ_e air and trigger deep convection in outer rainbands. There are two mechanisms proposed as to why the generation of spiral rainbands is important in the growth of a TC. In the experiments by Xu and Wang (2010), diabatic heating outside the eyewall decreased the stability of the atmosphere, owing to larger CAPE and higher production of spiral rainbands (Xu and Wang 2010). The theories by May and Holland (1999) and Hill and Lackmann (2009) suggest that spiral rainbands generate potential vorticity anomalies which merge with the stronger inner-core PV anomaly and cause radial expansion of the overall wind field. Since the stability of the environment remained essentially unchanged by changes in temperature in the simulations discussed here, it is more likely that size changes are due to PV generation.

Figure 2 shows the composite radar reflectivity at 24 h, 60 h, and 120 h into the simulation. Rainband features can be observed in all three environments by hour 24. However the extent of the precipitation field is largest in C3. There is little difference in intensity among the simulations by hour 60, yet C3 maintains the largest precipitation field, and continues to do so through hour 120. The rainband features in C3 at 60 h and 120 h extend further than the other simulations from the center of the storm, adding to the size of the precipitation field.

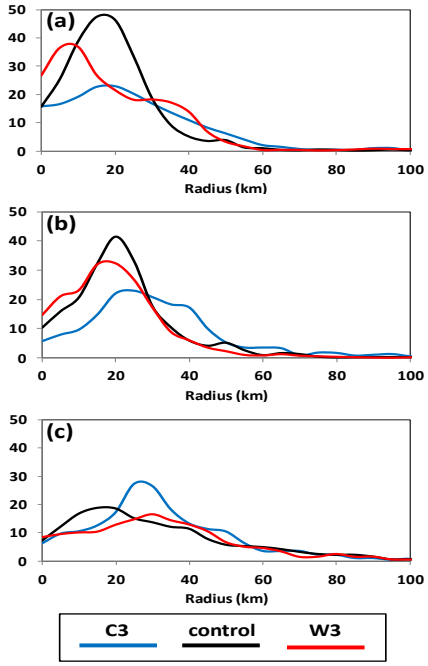

Figure 3. Azimuthally averaged 850-hPa PV (PVU, 1 PVU = 10^{-6} m^2 s^{-1} K kg^{-1}) versus radius for storms C3, control, and W3 at: a) 24 h; b) 60 h; and c) 120 h of the simulation.

In order to explore the potential relationship between outer rain bands, diabatic generation of PV, and outer wind field expansion, azimuthally-averaged plots of 850-hPa potential vorticity are shown in Figure 3 for the three simulations at three different times. At hour 24, the magnitude of the vorticity is highest in the control. C3 has lower peak magnitudes of PV, but higher values beyond about 30 km radius. A similar pattern occurs at hour 60. However, the "PV shoulder" in the C3 simulation is considerably larger than for the other two simulations. And it is around this time that the dramatic increase in the R34 for C3 begins. Despite the fact that the PV maximum is lower in C3 than in W3 and the control, the radial size of the PV field in C3 is much higher. Recalling that the wind field associated with a PV anomaly extends far beyond the anomaly itself, we can begin to see how these diabatically-generated PV bands influence the associated far-field winds, resulting in considerable extension of R34. At 120 hours, the magnitude of the PV is highest in C3 and lowest in W3. In addition, the size of the PV field is still slightly larger in C3. Figure 4 shows a horizontal cross-section of the 850-hPa PV at hour 60 for C3 and W3. These figures are consistent in showing that the magnitude of PV in the

inner-core is important in intensification, but the size of the PV field and radial extent of rainbands is important for the expansion of the wind field.

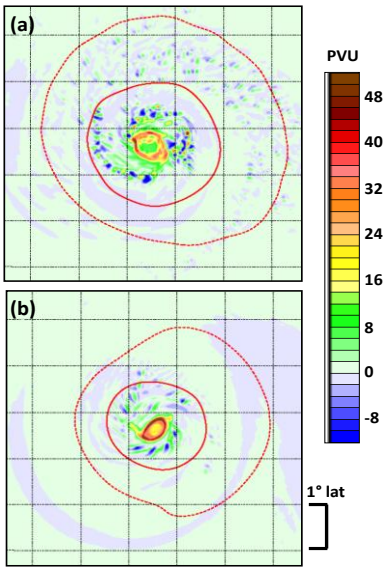

Figure 4. The domain 3 850-hPa potential vorticity at hour 60 for: a) C3; and b) W3. The red solid line indicates the extent of the 64-kt winds and the red dashed line indicates the extent of the 34-kt winds.

5. CONCLUSION

In this paper, three idealized simulations have been presented showing the influence of atmospheric temperature on the size and structure of tropical cyclones. The colder environment produced the largest and most intense tropical cyclone because the atmospheric temperature was cooler than the underlying sea-surface and the difference in the vapor pressure was larger, which led to enhanced surface moisture fluxes within the inner- and outer-core. The outer-core fluxes led to enhanced outer rainband generation, which led to higher PV generation in the outer-core and hence a larger wind field. These results are important because it shows that higher theta-e in the lower atmosphere (e.g., Stovern and Ritchie 2012) may not be as important as the amount of surface moisture fluxes during the growth of a TC. Although high boundary-layer θ_e air may be important for development of convection leading to intensification, once it is depleted, the moisture fluxes, specifically in the outer-core, are more important for rainband generation and expansion of the wind field.

Future work incudes exploring other potential mechanisms for the size growth of the simulated tropical cyclones including exploring angular momentum flux contributions to the outer wind field expansion. In addition, other simulations that further explore the relationship between SSTs, environmental temperature profiles and the static stability of the atmosphere are being analyzed.

Acknowledgements: This research was sponsored by the National Science Foundation Physical and Dynamical Meteorology Program under Grant #AGS-0822660.

6. REFERENCES

Beven, J. L., L. A. Avila, E. S. Blake, D.l P. Brown, J. L. Franklin, R. D. Knabb, R. J. Pasch, J. R. Rhome, and S. R. Stewart, 2008: Atlantic hurricane season of 2005. *Mon. Wea. Rev.*, **136**, 1109–1173.

Betts, A. K. 1987: Thermodynamic budget diagrams for the hurricane subcloud layer. *J. Atmos. Sci.*, **44**, 842-849.

Emanuel, K. A., 1986: An air-sea interaction theory for tropical cyclones. Part I: Steady state maintenance. *J. Atmos. Sci*., **43**, 585-604.

Frank, W. M. and E. A. Ritchie, 1999: Effects on environmental flow upon tropical cyclone structure. *Mon. Wea. Rev.,* **127**, 2044-2061.

Hill, K. A., G.M. Lackmann, 2009: Influence of Environmental Humidity on Tropical Cyclone Size. *Mon. Wea. Rev.*, **137**, 3294–3315.

Jaimes, B., and L. K. Shay, 2009: Mixed Layer Cooling in Mesoscale Oceanic Eddies during Hurricanes Katrina and Rita. *Mon. Wea. Rev.*, **137**, 4188–4207.

Malkus, J. S., and H. Riehl, 1960: On the dynamics and energy transformation in steady-state hurricanes. *Tellus*, **12**, 1-20.

May, P. T., and G. J. Holland, 1999: The role of potential vorticity generation in tropical cyclone rainbands. *J. Atmos. Sci.,* **56**, 1224-1228.

McBride, J. L., 1981a: Observational analysis of tropical cyclone formation. Part 1: Basic description of data sets. *J. Atmos. Sci.,* **38**, 1117-1131.

Skamarock, W. C., J. B. Klemp, J. Dudhia, D. O. Gill, D. M. Barker, W. Wang, and J. G. Powers, 2005: A description of the Advanced Research WRF Version 2. NCAR Tech Notes-468+STR. 88 pp.

Stovern, D. R. and E. A. Ritchie, 2012: How changes in atmospheric temperature affect the size and structure of tropical cyclones. *Revised for MWR.*